Inorg. Chem. **2008**, *47*, 8267−8277

Nanoparticulated Silicas with Bimodal Porosity: Chemical Control of the Pore Sizes

Jamal El Haskouri,* José Manuel Morales, David Ortiz de Zárate, Lorenzo Fernández, Julio Latorre, Carmen Guillem, Aurelio Beltrán, Daniel Beltrán,* and Pedro Amorós*

Institut de Ciència dels Materials de la Universitat de València (ICMUV), P.O. Box 22085, 46071-Valencia, Spain

Received May 16, 2008

Nanoparticulated bimodal porous silicas (NBSs) with pore systems structured at two length scales (meso- and large-meso-/macropores) have been prepared through a one-pot surfactant-assisted procedure by using a simple template agent and starting from silicon atrane complexes as hydrolytic inorganic precursors. The final bulk materials are constructed by an aggregation of pseudospherical mesoporous primary nanoparticles process, over the course of which the interparticle (textural) large pore system is generated. A fine-tuning of the procedural variables allows not only an adjustment of the processes of nucleation and growth of the primary nanoparticles but also a modulation of their subsequent aggregation. In this way, we achieve good control of the porosity of both the intra- and interparticle pore systems by managing independent variables. We analyze in particular the regulating role played by two physicochemical variables: the critical micelar concentration (cmc) of the surfactant and the dielectric constant of the reaction medium.

Introduction

High surface materials showing tailor-made pore sizes and shapes are especially interesting in a diversity of applications where molecular recognition is needed (shape-selective catalysis, molecular sieving, sensors, or selective adsorption, among others).[1] Although inorganic porous solids have been known for a long time, the research on porous materials chemistry was boosted in recent times by the discovery of the M41S silicas.[2] The introduction of surfactants as "templates" or "structure-directing agents" meant the opening of a novel pathway that permitted an expansion of the typical sizes of micropores in zeotypes to the mesopore range, which in turn implied an opportunity for new products and applications that explains the proliferation of mesoporous materials in recent years.[3]

A couple of decades (and thousands of reports) later, it could be thought that all has already been said about the chemistry of mesoporous materials. This is not so, despite having at our disposal a lot of information concerning, particularly, formally rather simple chemistry, the hydrolysis of siliceous and nonsiliceous alkoxides in hydroalcoholic media, which occurs in the presence of surfactant systems. Also, as suggested above, a key feature of these materials is, besides their ultimate composition and homogeneity, the set of structural parameters characterizing their topology (framework and texture). Among them, we can point out pore dimensions and arrays, wall thickness, crystalline order, and particle size. On the other hand, concerning preparative chemistry, we find in practice a huge collection of more or less rationalized recipes usually aimed at controlling some of these specific parameters (managing procedural variables like the type and concentration of precursors and surfactants, solvents, pH, temperature, or thermal treatments, among others),[1a,4] but an understandable chemical approach allowing the modulation of, to some extent, the material topology as a whole has not been clearly formulated yet.

* Authors to whom correspondence should be addressed. Phone: +34-96-3543617. Fax: +34-96-3543633. E-mail: pedro.amoros@uv.es (P.A.), daniel.beltran@uv.es (D.B.), haskouri@uv.es (J.E.H.).

(1) (a) Soler-Illia, G. J. A. A.; Sanchez, C.; Lebeau, B.; Patarin, J. *Chem. Rev.* **2002**, *102*, 4093. (b) Schüth, F.; Schmidt, W. *Adv. Mater.* **2002**, *14*, 629. (c) Davis, M. E. *Nature* **2002**, *417*, 813.

(2) Kresge, C. T.; Leonowicz, M. E.; Roth, W. J.; Vartuli, J. C.; Beck, J. S. *Nature* **1992**, *359*, 710.

(3) The Special Issue of Chemistry of Materials (Vol. 20, 2008) entitled Templated Materials constitutes a recent overview on the evolution of both the template concept and "surfactant assisted" syntheses.

(4) (a) Wan, Y.; Zhao, D. Y. *Chem. Rev* **2007**, *107*, 2821, and references therein. (b) Lin, H.-P.; Mou, C.-Y. *Acc. Chem. Res.* **2002**, *35*, 927.

10.1021/ic800893a CCC: $40.75
Published on Web 08/14/2008

Although it was initially considered that the intermediate mesostructures resulted from the growth of an inorganic phase in the interstices (intermicellar space) of a previously formed ordered organic mesophase (LCT mechanism),[2] nowadays it is fully demonstrated that the pre-existence of a liquid-crystal-like templating phase is not necessary at all. In practice, most of the described mesostructures have been prepared using surfactant concentrations above the corresponding value of the critical micelar concentration (cmc) but notably lower than those required for the formation of liquid crystal phases.[5] In any case, the study of the possible reaction mechanisms has remained a very active research field over the course of time. Thus, *in situ* experimental studies at different length and time scales have been published (1) at the molecular level on the precursor solutions by using spectroscopic methods,[6] (2) on the mesoscopic scale during mesostructure formation (transmission electron microscopy (TEM), small angle X-ray scattering, etc.),[7] and (3) on the macroscopic scale after mesostructure stabilization and long-range order was achieved.[8]

Regardless of what the ultimate mechanistic details may be, it is currently accepted that mesostructure formation implies the cooperative self-assembling of organic and inorganic supramolecular moieties which, without prejudice to the above, generates entities organized under arrays similar to those typical of the pure tensoactive mesophases. In other words, the active organic species ("templates" or "structure-directing agents") in the formation of a mesostructure are surfactant micelles (neutral or not), which constitute therefore a necessary starting point in the material formation.[5−8] The inorganic counterpart, monomeric or oligomeric species resulting from hydrolytic condensation processes, incorporates to the micelle surface (van der Waals or electrostatic forces), this making feasible the directed progress of subsequent condensations leading finally to the solid structure. Thus, mesostructured materials can be considered to be hybrid (organic−inorganic) composites in which each component (micelles and oligomers) comes from the independent development of its own chemistry. We will return to this matter later on.

Our group has proven expertise in synthesizing varied mesoporous materials displaying different textural features.[9] In accordance with the above, our experience indicates that any effort to understand and, therefore, intend to manage at convenience the preparation of mesoporous materials should be focused on the capability of harmonizing the equilibrium reactions' evolution involving each one of the reactive species (tensoactive molecules/micelles and precursors/oligomers). Indeed, the precipitation of an intermediate siliceous crystalline mesostructure from solution (without prejudice to using biphasic reaction media) proceeds through the formation of adducts of supramolecular species and is obviously governed by the principles of a solubility (pseudo) equilibrium (lattice energy/solvation phenomena). It seems also evident that the effective driving force of the final precipitation of any siliceous mesostructure is the essentially irreversible condensation of the inorganic moiety. Under this assumption, we could alter the topologic features of the final material insofar as we were able to modulate parameters affecting the particle-nucleation and growing stages, that is to say, the formation and evolution of the micelles−oligomers adducts. This point will constitute a central part of the present report.

In the never-ending dialectic between prospects for utility and performance indicators, the interest of many research groups in the required topologic features of high surface mesoporous materials has covered all corners: from the structural appeal of the ordered mesopore arrays with narrow pore size distributions characterizing the M41S-related derivatives to the search for frameworks including pore systems hierarchically structured under complex macroscale forms.[10] It has been argued that a periodic and unimodal mesoporous structure could not offer specific advantages for certain applications since the bulk materials might suffer from hindered accessibility to the active sites because of partial

(5) (a) Huo, Q.; Margolese, D.; Ciesla, U.; Demuth, D. G.; Feng, P.; Gier, T. E.; Sieger, P.; Firouzi, A.; Chmelka, B. F.; Schuth, F.; Stucky, G. D. *Chem. Mater.* **1994**, *6*, 1176. (b) Monnier, A.; Schüth, F.; Huo, Q.; Kumar, D.; Margolese, D.; Maxwell, R. S.; Stucky, G. D.; Krishnamurty, M.; Petroff, P.; Firouzi, A.; Janicke, M.; Chmelka, B. F. *Science* **1993**, *261*, 1299. (c) Chen, C. Y.; Burkett, S. L.; Li, H. X.; Davis, M. E. *Microporous Mater.* **1993**, *2*, 27. (d) Vartuli, J. C.; Kresge, C. T.; Leonowicz, M. E.; Chu, A. S.; McCullen, S. B.; Johnson, I. D.; Sheppard, E. W. *Chem. Mater.* **1994**, *6*, 2070. (e) Beck, J. S.; Vartuli, J. C.; Kennedy, G. J.; Kresge, C. T.; Roth, W. J.; Schramm, S. E. *Chem. Mater.* **1994**, *6*, 1816. (f) Firouzi, A.; Kumar, D.; Bull, L. M.; Besier, T.; Sieger, P.; Huo, Q.; Walker, S. A.; Zasadzinski, J. A.; Glinka, C.; Nicol, J.; Margolese, D.; Stucky, G. B.; Chmelka, B. F. *Science* **1995**, *267*, 1138.

(6) (a) Calabro, D. C.; Valyocsik, E. W.; Ryan, F. X. *Microporous Mater.* **1996**, *7*, 243. (b) Firouzi, A.; Atef, F.; Oertli, A. G.; Stucky, G. D.; Chmelka, B. F. *J. Am. Chem. Soc.* **1997**, *119*, 3596. (c) Galarneau, A.; Renzo, F. D.; Fajula, F.; Mollo, L.; Fubini, B.; Ottaviani, M. F. *J. Colloid Interface Sci.* **1998**, *201*, 105–107. (d) Holmes, S. M.; Zholobenko, V. L.; Thursfield, A.; Plaisted, R. J.; Cundy, C. S.; Dwyer, J. *J. Chem. Soc., Faraday Trans.* **1998**, *94*, 2025. (e) Melosh, N. A.; Lipic, P.; Bates, F. S.; Wudl, F.; Stucky, G. D.; Fredrickson, G. H.; Chmelka, B. F. *Macromolecules* **1999**, *32*, 4332. (f) Zhang, J.; Luz, Z.; Zimmermann, H.; Goldfarb, D. *J. Phys. Chem. B* **2000**, *104*, 279. (g) Frasch, J.; Lebeau, B.; Soluard, M.; Patarin, J.; Zana, R. *Langmuir* **2000**, *16*, 9049. (h) Zhang, J.; Goldfarb, D. *Mesoporous Mater.* **2001**, *48*, 143–149. (i) Boissiere, C.; Larbot, A.; Bourgaux, C.; Prouzet, E.; Bunton, C. A. *Chem. Mater.* **2001**, *13*, 3580. (j) Zhang, J.; Carl, P. J.; Zimmermann, H.; Goldfarb, D. *J. Phys. Chem. B* **2002**, *106*, 5382. (k) Ruthstein, S.; Frydman, V.; Kababya, S.; Landau, M.; Goldfarb, D. *J. Phys. Chem. B* **2003**, *107*, 1739. (l) Ruthstein, S.; Frydman, V.; Goldfarb, D. *J. Phys. Chem. B* **2004**, *108*, 9016. (m) Ottaviani, M. F.; Moscatelli, A.; Desplantier-Giscard, D.; Di Renzo, F.; Kooyman, P. J.; Alonso, B.; Galarneau, A. *J. Phys. Chem. B* **2004**, *108*, 12123. (n) Flodström, K.; Wennerström, H.; Alfredsson, V. *Langmuir* **2004**, *20*, 680. (o) Flodström, K.; Teixeira, C. V.; Amenitsch, H.; Alfredsson, V.; Lindén, M. *Langmuir* **2004**, *20*, 4885. (p) Baccile, N.; Laurent, G.; Bonhomme, C.; Innocenzi, P.; Babonneau, F. *Chem. Mater.* **2007**, *19*, 1343.

(7) (a) Regev, O. *Langmuir* **1996**, *12*, 4940. (b) Lindén, M.; Schunk, S. A.; Schüth, F. *Angew. Chem., Int. Ed. Engl.* **1998**, *37*, 6–821. (c) Adachi, M.; Murata, Y.; Sago, K.; Nakagawa, K. *Langmuir* **2004**, *20*, 5965.

(8) See for example: Yu, C.; Fan, J.; Tian, B.; Zhao, D. *Chem. Mater.* **2004**, *16*, 889.

(9) (a) Cabrera, S.; El Haskouri, J.; Alamo, J.; Beltrán, A.; Beltrán, D.; Mendioroz, S.; Marcos, M. D.; Amorós, P. *Adv. Mater.* **1999**, *11*, 379. (b) Cabrera, S.; El Haskouri, J.; Guillem, C.; Beltrán, A.; Beltrán, D.; Mendioroz, S.; Marcos, M. D.; Amorós, P. *Chem. Commun.* **1999**, 333. (c) El Haskouri, J.; Cabrera, S.; Caldés, M.; Alamo, J.; Beltrán, A.; Marcos, M. D.; Amorós, P.; Beltrán, D. *Int. J. Inorg. Mater* **2001**, *3*, 1157. (d) El Haskouri, J.; Cabrera, S.; Caldés, M.; Guillem, C.; Latorre, J.; Beltrán, A.; Beltrán, D.; Marcos, M. D.; Amorós, P. *Chem. Mater.* **2002**, *14*, 2637. (e) El Haskouri, J.; Latorre, J.; Guillem, C.; Beltrán, A.; Beltrán, D.; Amorós, P. *Chem. Mater.* **2004**, *16*, 4359.

or total pore-blocking phenomena.[11] In this sense, the presence of pore systems structured at different length scales could offer the possibility of combining an enhanced accessibility to the functional active groups (across large pores) with the conservation of high surface area and pore volume.[12,13] One of the alternative ways to deal with the site accessibility (or diffusion constraints) problem is conceptually based on the consequences of decreasing (at the nanoparticle range) the particle size of the mesoporous material. This necessarily implies, at first, the shortening of the mesopore length, whereas the nanoparticle packing would generate supplementary interparticle (textural) porosity.[14]

As a matter of fact, the synthesis of nanoparticulated bimodal mesoporous silica (NBS) materials has aroused great interest in recent years.[15] As commonly occurs in the synthesis of mesoporous materials, the surfactant-assisted procedures describing the preparation of NBS associate their ability for yielding these type of materials with a diversity of experimental factors (polarity of the medium, pH of the mother solution, concentration, etc.), which, in the case we are dealing with, would limit the growth of the mesoporous silica particles and would regulate their aggregation processes.[15] Also, attention has been paid to recipes allowing the achievement of good control of the pore sizes. Thus, it has been stated that it should be possible to modify the interparticle (textural) pore size by controlling procedural variables such as the gel time or the surfactant concentration or by using two surfactant types.[15] On the other hand, the possibility of modulating the intraparticle mesopore sizes by using alkylammonium surfactants with variable tail lengths has been recently reported.[16] However, as far as we know, there is no report in the literature concerning the feasibility of controlling the sizes of both pore types in a given NBS family.

Here, we present for the first time a reproducible synthesis procedure allowing the independent control of both the intra- and interparticle pore systems in NBS materials. Besides the inherent interest in these materials, our main goal is to corroborate that, by a fine-tuning of the procedural variables, a well-defined and simple synthesis strategy can lead to mesoporous silicas showing significantly different topologic features. As indicated above, our attention will be focused on the capability of orchestrating the equilibriums involving each one of the active species (micelles and oligomers) in such a way that the aggregation of the structural building blocks evolves until the controlled NBS formation is achieved. We have been able to do it by efficiently regulating two physicochemical procedural variables: the concentration of the surfactant and the dielectric constant of the reaction medium.

Experimental Section

Synthesis. The method is a modification of the so-called "atrane route", which is based on the use of (1) a hydroalcoholic reaction medium that, among other functions, allows the existence of "atranes" (i.e., complexes that include triethanolamine-related ligand species) as hydrolytic inorganic precursors and (2) a cationic surfactant as a structural directing agent or supramolecular template and, consequently, as a porogen after template removal. Details of the "atrane route", as well as its versatility to yield a diversity of mesoporous materials, have been reported elsewhere.[17]

Chemicals. All the synthesis reagents are analytically pure and were used as received from Aldrich (tetraethyl orthosilicate (TEOS), triethanolamine [$N(CH_2-CH_2-OH)_3$, hereinafter TEAH3], octadecyl-trimethylammonium bromide (C_{18}TMABr), cetyl-trimethylammonium bromide (C_{16}TMABr), tetradecyl-trimethylammonium bromide (C_{14}TMABr), dodecyl-trimethylammonium bromide (C_{12}TMABr), decyl-trimethylammonium bromide (C_{10}TMABr), and ethanol).

Preparative Procedure. All of the samples reported in this publication were prepared by the same general method, and using molar ratios of the reagents in the mother solution according to: 2 Si/7 TEAH3/*y* C_xTMABr/*z* ethanol/*w* H_2O (where *x* refers to the number of carbon atoms in the surfactant tail). The TEAH3, which is in excess with regard to the amount required to form silatranes (mainly in the form of Si(TEA)(TEAH$_2$)),[17,18] also acts as a cosolvent.

In order to control the intraparticle pore system, we used surfactants with different tail lengths (Table 1). In this case, the molar ratio of the reagents in the mother solution was adjusted to 2 Si/7 TEAH3/*y* C_xTMABr/180 H_2O. That is to say, we used variable amounts (*y*) of the surfactants in the absence of ethanol ($z = 0$). The amount of surfactant (*y*) was increased as the tail length (*x*) decreased. Such a variation had the objective of maintaining surfactant concentrations in the mother solution a little higher than those corresponding to the respective cmc values:[19,20] 0.2 ($x = 18$), 0.5 ($x = 16$), 2 ($x = 14$), 8 ($x = 12$), and 32 ($x = 10$). In a typical one-pot synthesis leading to sample 4, a mixture of TEOS (10.7 mL, 0.05 mol) and liquid TEAH3 (22.3 mL, 0.17 mol) was heated at 150 °C for 10 min in order to form silatrane complexes in a TEAH3 medium. The resulting solution was cooled down to

(10) (a) Zhang, B.; Davis, S. A.; Mann, S. *Chem. Mater.* **2002**, *14*, 1369. (b) Kuang, D.; Brezesinski, T.; Smarsly, B. *J. Am. Chem. Soc.* **2005**, *17*, 1683. (c) Tosheva, L.; Valtchev, V.; Sterte, J. *Microporous Mesoporous Mater.* **2000**, *35*−*36*, 621. (d) Blanford, C. F.; Yan, H.; Schroden, R. C.; Al-Douas, M.; Stein, A. *Adv. Mater.* **2001**, *13*, 401. (e) Sen, T.; Tiddy, G. J. T.; Casci, J. L.; Anderson, M. W. *Chem. Mater.* **2004**, *16*, 2044. (f) Imhof, A.; Pine, D. J. *Nature* **1997**, *389*, 948. (g) Caruso, R. A.; Antonietti, M. *Adv. Funct. Mater.* **2002**, *12*, 307. (h) Stein, A.; Li, F.; Denny, N. R. *Chem. Mater.* **2008**, *20*, 649.
(11) Rolison, D. R. *Science* **2003**, *299*, 1698.
(12) Antonietti, M.; Ozin, G. A. *Chem.*−*Eur. J.* **2004**, *10*, 28.
(13) Yuan, Z.; Su, B.-L. *J. Mater. Chem.* **2006**, *16*, 663.
(14) El Haskouri, J.; Ortiz de Zárate, D.; Guillem, C.; Latorre, J.; Caldés, M.; Beltrán, A.; Beltrán, D.; Descalzo, A. B.; Rodríguez, G.; Martínez, R.; Marcos, M. D.; Amorós, P. *Chem. Commun.* **2002**, 330.
(15) (a) Zhang, W.; Pauly, T. R.; Pinnavaia, T. J. *Chem. Mater.* **1997**, *9*, 2491. (b) Sun, J.; Shan, Z.; Maschmeyer, T.; Coppens, M.-O. *Langmuir* **2003**, *19*, 8395. (c) Lin, H.-P.; Tsai, C.-P. *Chem. Lett.* **2003**, *32*, 1092. (d) Smått, J.-H.; Schunk, S.; Lindén, M. *Chem. Mater.* **2003**, *15*, 2354. (e) Lee, J.; Kim, J.; Hyeon, T. *Chem. Commun.* **2003**, 1138. (f) Suzuki, K.; Ikari, K.; Imai, H. *J. Am. Chem. Soc.* **2004**, *126*, 462. (g) Chao, M.-C.; Lin, H.-P.; Mou, C. Y. *Chem. Lett.* **2004**, *33*, 672. (h) Wang, X.; Li, W.; Zhu, G.; Qiu, S.; Zhao, D.; Zhong, B. *Microporous Mesoporous Mater.* **2004**, *71*, 87. (i) Ikari, K.; Suzuki, K.; Imai, H. *Langmuir* **2006**, *22*, 802.
(16) Huerta, L.; Guillem, C.; Latorre, J.; Beltrán, A.; Martínez-Máñez, R.; Marcos, M. D.; Beltrán, D.; Amorós, P. *Solid State Sci.* **2006**, *8*, 940.
(17) Cabrera, S.; El Haskouri, J.; Guillem, C.; Latorre, J.; Beltrán, A.; Beltrán, D.; Marcos, M. D.; Amorós, P. *Solid State Sci.* **2000**, *2*, 405.
(18) Fernandez, L.; Viruela-Martin, P.; Latorre, J.; Guillem, C.; Beltrán, A.; Amorós, P. *THEOCHEM* **2007**, *822*, 89.
(19) Laughlin, R. G. *The Aqueous Phase Behavior of Surfactants*; Academic Press: San Diego, CA, 1994.
(20) (a) Hunter, R. J. *Foundations of Colloid Science*; Academic Press: New York, 1993; p 569. (b) Klevens, H. B. *J. Am. Oil Chem. Soc.* **1953**, *30*, 74.

Table 1. Selected Preparative and Physical Data for UVM-7 Silicas with Tailored Intraparticle Mesopore System

					pore systems			
					intraparticle mesopore system		interparticle large pore system	
sample	C_xTMABr/x[a]	C_xTMABr/y[b]	a_0[c]/nm	surface[d]/m^2/g	size[e]/nm	volume[e]/cm^3/g	size[e]/nm	volume[e]/cm^3/g
1	10	32	4.04	1128	1.81	0.35	45.0	1.48
2	12	8	4.24	1279	2.11	0.75	53.2	1.26
3	14	2	4.59	1088	2.56	0.87	55.5	1.0
4	16	0.5	5.28	1105	3.02	0.98	49.0	1.41
5	18	0.2	5.87	1050	3.41	1.04	51.7	1.30

[a] Surfactant tail length: x = number of carbon atoms. [b] Surfactant molar concentration according to 2 Si/7 triethanolamine/y C_xTMABr/180 H_2O. [c] Cell parameters calculated assuming an MCM-41-like hexagonal cell ($a_0 = 2d_{100}/3^{1/2}$). [d] Surface area according to the BET model. [e] Pore diameters and volumes calculated by using the BJH model on the adsorption branch of the isotherms.

Table 2. Selected Preparative and Physical Data for UVM-7 Silicas with Tailored Interparticle Pore System

					pore systems			
					intraparticle mesopore system		interparticle large pore system	
sample	ethanol/z[a]	a_0[b]/nm	particle/nm[c]	surface[d]/m^2/g	size[e]/nm	volume[e]/cm^3/g	size[e]/nm	volume[e]/cm^3/g
6	3	4.85	25−35	1228	3.04	1.02	50.1	1.51
7	5	4.97	30−50	1152	3.00	0.89	55.3	0.47
8	10	4.74	100−200	1111	2.77	0.90	58.0	0.15
9	40	4.54	400−500	1123	2.56	0.80		
10	50	4.25	600−1000	1155	2.43	0.84		

[a] Ethanol molar concentration (z) according to 2 Si/7 triethanolamine/0.52 $C_{16}TMABr$/z ethanol/180 H_2O. [b] Cell parameters calculated assuming a MCM-41-like hexagonal cell ($a_0 = 2d_{100}/3^{1/2}$). [c] Averaged particle size ranges from TEM and/or SEM. [d] Surface area according to the BET model. [e] Pore diameters and volumes calculated by using the BJH model on the adsorption branch of the isotherms

Table 3. Selected Preparative and Physical Data for UVM-7 Silicas with Ordered Intraparticle Mesopore System

					pore systems			
					intraparticle mesopore system		interparticle large pore system	
sample	water/w[a]	a_0[b]/nm	particle/nm[c]	surface[d]/m^2/g	size[e]/nm	volume[e]/cm^3/g	size[e]/nm	volume[e]/cm^3/g
11	640	4.85	40−60	898	2.75	0.67	55.2	0.74
12	2880	4.97	50−70	981	2.77	0.63	57.1	0.71

[a] Water molar concentration (w) according to 0.52 $C_{16}TMABr$/w H_2O. [b] Cell parameters calculated assuming a MCM-41-like hexagonal cell ($a_0 = 2d_{100}/3^{1/2}$). [c] Averaged particle size ranges from TEM. [d] Surface area according to the BET model. [e] Pore diameters and volumes calculated by using the BJH model on the adsorption branch of the isotherms.

90 °C, and 4.56 g of $C_{16}TMABr$ (0.0125 mol) was added. Then, 80 mL of water was slowly added with vigorous stirring at a mixing temperature of 80 °C. After a few minutes, a white suspension resulted. This mixture was allowed to age at room temperature for 4 h. The resulting mesostructured powder was separated by filtration or centrifugation, washed with water and ethanol, and air-dried. In order to prepare the final porous material, the surfactant was removed from the mesostructure by calcination (540 °C for 4 h under static air atmosphere).

On the other hand, in order to modulate the nanoparticles' aggregation processes (and, consequently, the interparticle or textural porosity), we modified the dielectric constant of the reaction medium by adding variable amounts of ethanol. Now, the molar ratio of the reagents was 2 Si/7 TEAH3/y C_xTMABr/z ethanol/180 H_2O. Summarized in Table 2 are the preparative conditions referred to a given family ($x = 16$, $y = 0.5$) of NBS samples. As can be observed, the z value was varied from 3 to 50. The $z = 0$ case would correspond to sample 4. In a typical synthesis leading to sample 8, we applied exactly the same procedure described above for sample 4 until the step corresponding to the surfactant addition was reached. Then, a mixture of 11.4 mL of ethanol and 80 mL of water was added under stirring at 80 °C. A white solid appeared, and it was separated and treated as described above.

An additional observation was the fact that the relative symmetry of the mesopore intraparticle system can be enhanced working under high dilutions (Table 3). Then, samples 11 and 12 were prepared following exactly the same protocol that we have used for sample 4, but adding significantly higher water amounts ($w = 640$ and 2880 instead of 180). In all cases, we have detailed here syntheses involving $C_{16}TMABr$ (cetyl-trimethylammonium bromide), the commercial surfactant most widely used in the synthesis of porous materials.

Physical Measurements. All solids were characterized by X-ray powder diffraction (XRD) at low angles (Seifert 3000TT θ-θ) using Cu Kα radiation. Patterns were collected in steps of 0.1° (2θ) over the angular range 1.5−7.0 for 10 s per step. An electron microscopy study (TEM) was carried out with a JEOL JEM-1010 instrument operating at 100 kV and equipped with a CCD camera. Samples were gently ground in dodecane, and microparticles were deposited on a holey carbon film supported on a Cu grid. Scanning electron microscopy (SEM) images were recorded using a Hitachi S-4100 FE microscope. Samples were previously coated with Au−Pd. Surface area, pore size, and volume values were calculated from nitrogen adsorption−desorption isotherms (−196 °C) recorded on a Micromeritics ASAP-2010 automated analyzer. Calcined samples were degassed for 5 h at 120 °C and 10^{-6} Torr prior to analysis. Surface areas were estimated according to the Brunauer−Emmett−Teller (BET) model, and pore size dimensions and pore volumes were calculated by using the Bopp−Jancso−Heinzinger (BJH) method from the absorption branch of the isotherms.

Results and Discussion

Synthesis Strategy. Following previous work on related UVM-*n* material series (for University of Valencia Materials-*n*), we succeeded in synthesizing a novel NBS family (denoted as UVM-7).[14,16] Our synthesis strategy for obtaining the original UVM-7 materials was an application of the so-

called "atrane route" based on using silatrane precursors and a cationic surfactant (cetyltrimethylammonium bromide or related species, hereafter, C_xTMABr). This strategy is based on the use of atrane complexes as inorganic hydrolytic precursors. Atranes are a specific type of alkoxo complex including triethanolamine-like species acting as anionic tripod ligands, whose name corresponds to an acronym of AminoTRiethoxymetallANES. Atrane complexes are, in general, unstable but relatively inert toward hydrolysis, which aids the orchestration of the self-assembling processes (between the inorganic moieties and the surfactant aggregates) that lead to stable mesostructured phases. The general aspects of the procedure for synthesizing the NBS materials described here coincide with those previously reported,[17] except for some modifications specified in the experimental section and discussed below.

Once the silatranes (mainly in the form of Si(TEA)-($TEAH_2$)) were formed, our syntheses started from homogeneous solutions containing these precursor species and the surfactant. In general, under the working conditions, the solutions will contain surfactant micelles in dynamic equilibrium with a constant concentration of surfactant monomers (cmc).[19] Then, water addition provokes the hydrolysis and subsequent condensation of the silica precursor, which generates supramolecular inorganic fragments (oligomers) in the presence of the pre-existent micelles. At some point in the course of these hydrolytic processes, we would have in solution anionic oligomers adequate to adhere to the surface of the cationic micelles because of electrostatic forces (taking eventually the place of pre-existent bromide counterions). In any case, whatever the silicon source may be, the self-assembling processes initiating the formation of mesostructured silica particles (i.e., the interactions finally responsible for the intraparticle pores) depend on the adequate charge-matching between anionic silica oligomers and cationic micelles. Now, the subsequent condensations of siliceous oligomers (an essentially irreversible process) will occur on the external surface of the micelles, which will result in rigid hybrid (silicate-coated) micelar entities unfit for exchanging tensoactive monomers with the mother solution. The hybrid-micelle concept was proposed by Boissiere et al.,[6i] dealing with the preparation of MSU-X mesoporous silicas. There are these rigid hybrid micelles which must aggregate and flocculate once attaining a size preventing their presence as colloidal particles in solution. Thus, we can say that mesostructured materials are hybrid (organic−inorganic) composites in which each component (micelles and silica oligomers) comes from the independent development of its own chemistry. In the simplest model of crystal growth, any hybrid micelle would correspond to the "embryos" concept. Otherwise, although they are unable to solve-back in their components, the "nuclei of critical size" must contain a finite number of ordered micelles in order to account for the crystalline structure. Insofar as the attractive forces among these hybrid or composite micelles have the same anisotropy as those working in the case of pure tensoactive micelles, we can understand their capability to originate similar liquid-crystal-like mesophases.

According to the above, we can propose that the formation of a solid siliceous mesostructure conceptually responds to a reaction of precipitation (without prejudice to the existence of a complex sequential mechanism):

$$(Si_{n+m}O_{3/2(n+m)}(OH)_nO_m)^{m-}\ \text{soln} + (C_xTMA^+Br^-)_m\ \text{soln} \rightarrow [(C_xTMA)_mSi_{n+m}O_{3/2(n+m)}(OH)_nO_m]\text{solid} + mBr^-\ \text{soln} \quad (1)$$

As far as we were able to control the evolution (kinetics) of this reaction, we could lead it toward the formation of nanoparticles. The heterogeneous final state could be ideally described as a solution (including cosolvent species) containing any excess of silica (more or less condensed) and surfactant molecules (cmc), together with the insoluble solid mesostructure.

As suggested above, the common objective in all of the procedures described in previous works for synthesizing NBS is to regulate the evolution of equilibrium 1 in such a way that the growth and aggregation of the resulting silica particles becomes hindered. If so, the nucleated primary nanoparticles would constitute the structural building blocks whose packing will define the textural large pores. Assuming an S^+I^- formation mechanism like the above, there is a certain agreement about the kinetic requirements favoring the NBS formation: the particle nucleation processes must be fast, and the subsequent condensation processes also must be fast to avoid the growth of large particles.[16] What we need in order to satisfy these requirements is to have at our disposal high concentrations of both reagents (silica oligomers and surfactant micelles) in the reaction medium. In short, dealing with the inorganic species, the NBS formation requires that (a) the hydrolysis of the silicon species (eqs 2 and 3) must be fast to achieve monomer supersaturation, (b) the subsequent condensation processes (eq 4) also must be fast to provide a high concentration of charged silica oligomers adequate to interact with C_xTMA^+ ions, and (c) the growth of large particles must be avoided working under conditions in which silica back-solution is restricted.

$$Si(TEA)_2H_2 + 4H_2O \rightarrow Si(OH)_4 + 2TEAH_3 \quad (2)$$

$$Si(OH)_4 + OH^- \leftrightarrow [Si(OH)_3O^-] + H_2O \quad (3)$$

$$n\text{Si(OH)}_4 + m[\text{Si(OH)}_3\text{O}^-] \leftrightarrow [\text{Si}_{n+m}\text{O}_{3/2(n+m)}(\text{OH})_n\text{O}_m]^{m-} + 3/2(n+m)\ \text{H}_2\text{O} \quad (4)$$

As demonstrated in refs 14 and 16, all of these requirements are satisfied under moderate basic conditions (pH ca. 9). Thus, the pH of the mother solution constitutes a procedural key for obtaining the UVM-7 silicas owing to the true nature of the hydrolytic processes involving the silicon moieties. In practice, by using the "atrane route", we ensure the adequate control of the pH conditions due to the buffering effect of triethanolamine, which stabilizes the working pH around 9. Then, we can say that triethanolamine plays an indirect role in the formation of the nanoparticulated UVM-7 bimodal porous silicas maintaining the reaction medium in the homogeneous phase and acting as a buffer

agent. Although UVM-7-related silicas can be synthesized from other inorganic precursors (TEOS or sodium silicate in the absence of triethanolamine), from the procedural point of view, the "atrane route" is extremely straightforward, allowing a fine control of the key parameter (pH), with the subsequent high reproducibility.

Dealing with the organic counterpart, it must be emphasized that the formation of the active species in these processes, micellar aggregates, requires surfactant concentrations above the corresponding cmc values. Once the critical value is achieved, the formation of micelles starts and progresses for increasing concentrations, while the tensoactive monomer concentration remains constant (around cmc). In the case of alkyltrimethilammonium surfactants, there is no dependence of cmc on the pH. In contrast to the pure tensoactive mesophases, it is the progress of the silicate condensation which acts as the driving force, leading to the irreversible formation and aggregation of hybrid micelles. It must also be noted that the chemical activity of the hybrid micelles (silicate-coated) with regard to the surfactant solution is null (the practical "sequestration" of the micelles breaks the dynamical equilibrium), which results in a practically constant concentration of nonaggregate surfactant molecules in solution (inadequate to give additional micelles). In the limit, all of the hybrid micelles would incorporate to the solid phase, and these micelles (in a finite number) are identifiable as structural blocks (i.e., they are not only kinetically relevant entities but also true structural units in the final material).

With all above considerations in mind, we have carried out different preparations whose goal is not only to obtain NBS materials but also to modulate their topologic features, mainly to control the porosity of both the intra- and the interparticle pore systems. We have put in use variables like the surfactant tail length and concentration, as well as the effect of using ethanol as cosolvent. It must be emphasized that the resource of these tools is based on general principles affecting the equilibrium like the proper cmc concept or the dependence of the solubility on the dielectric constant of the medium.

Intraparticle Mesopore Control. As mentioned above, we had investigated previously the possibility of modulating the intraparticle mesopore size in a given NBS family by using surfactants with variable hydrophobic tail lengths, while maintaining the same headgroup (C_xTMABr, $10 \leq x \leq 18$).[16] As expected, such a procedure (already checked for MCM-41 and related materials)[21] resulted in a stepped modulation of the intra-nanoparticle mesopore system. Unfortunately, the changes in the surfactant tail length also induced significant changes in the interparticle large-pore system. Indeed, as the surfactant tail length decreases, this additional (textural) porosity typical of the NBS materials ends up disappearing, which reflects the pronounced increase of the size of the nucleated primary particles (from 15 to 300 nm). Then, materials prepared using surfactants with short tail lengths ($x \leq 14$) showed MCM-41-like morphologies (Figure 1a,b). The NBS organization was only preserved when large surfactants ($x \geq 16$) were used as templates, as can be observed in Figure 1d,e.[16]

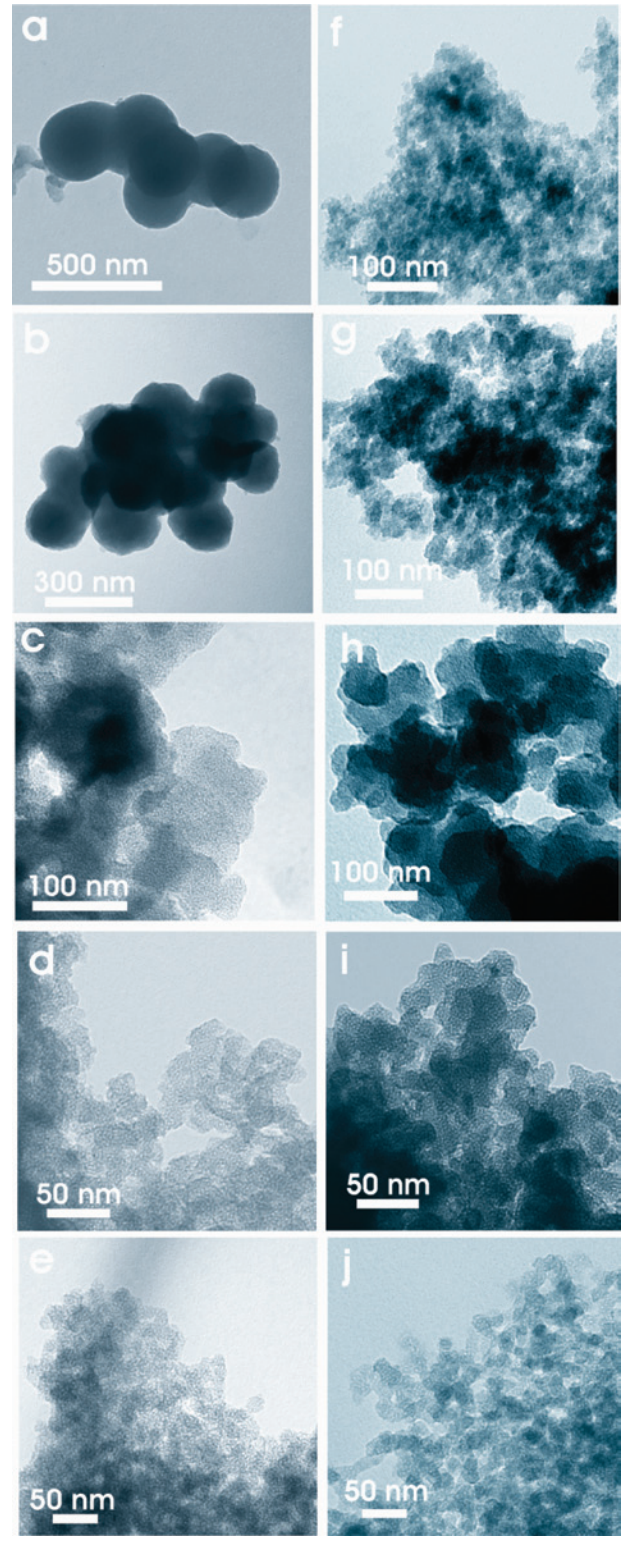

Figure 1. (a−e) TEM images of mesoporous silicas prepared at constant surfactant concentration (0.5 C_xTMABr/180 H_2O). (f−j) TEM micrographs of NBS synthesized at constant micelle concentration [(f) sample 1, (g) sample 2, (h) sample 3, (i) sample 4, (j) sample 5]. The surfactant C_xTMABr is (a, f) $x = 10$, (b, g) $x = 12$, (c, h) $x = 14$, (d, i) $x = 16$, and (e, j) $x = 18$.

(21) Beck, J. S.; Vartuli, J. C.; Roth, W. J.; Leonowicz, M. E.; Kresge, C. T.; Schmitt, K. D.; Chu, C. T.-W.; Olson, D. H.; Sheppard, E. W.; McCullen, S. B.; Higgins, J. B.; Schlenker, J. L. *J. Am. Chem. Soc.* **1992**, *114*, 10834.

The key to overcoming this problem, that is, to achieving a step-by-step modulation of the intraparticle mesopores without a loss of the NBS character, is implicit in equilibrium 1. Thus, as commented above, the organic species implied in the equilibrium really are micelles ($(C_xTMA^+Br^-)_m$) and not surfactant molecules ($mC_xTMA^+Br^-$). Accordingly, to preserve the NBS morphology, we must guarantee in all cases (surfactants) the presence of adequate concentrations of $(C_xTMA^+Br^-)_m$ micelles in solution, which can be achieved using surfactant concentrations slightly higher than the corresponding value of the cmc. In this sense, it is well known that the cmc of the surfactants increases as the tail length decreases,[19] but this relationship has not been taken into account usually (at least explicitly) in order to choose the surfactant concentration range in the synthesis of mesoporous oxides. In fact, in the case of surfactant concentrations such as that used in ref 16 (0.5 C_xTMABr/180 H_2O), the existence of micelles can be discarded for $x \leq 14$, which prevents the quick and massive nanoparticle nucleation required to produce NBS materials.

In order to preserve the NBS architecture, we have reformulated here our synthesis procedure in such a way that it is the micelle concentration of the different C_xTMABr ($10 \leq x \leq 18$) surfactants which remains constant (instead of the surfactant concentration). Thus, starting from the experimentally optimized value of the surfactant concentration for the $C_{16}TMABr$ case (0.5 $C_{16}TMABr$/180 H_2O), and taking into account the cmc values corresponding to the different C_xTMABr ($10 \leq x \leq 18$) surfactants,[19,20] we have calculated the amounts of surfactant which are necessary to maintain the micelle concentration in the mother liquor (Table 1).

As can be observed, the required surfactant amount increases in an exponential way as the surfactant tail length decreases. The result is that, on the basis of the cmc dependence on the surfactant tail length, we have made use in some cases of surfactant amounts that never have been explored in the literature (where only small variations of the surfactant concentration have been considered).[15]

TEM images in Figure 1 clearly show how the NBS architecture typical of the UVM-7 silicas is now preserved regardless the surfactant chain length (see Figure 1f−j). In all cases, the final materials can be described as bimodal porous silicas constructed by the aggregation of pseudospherical mesoporous primary nanoparticles. Both TEM images and XRD patterns indicate that the intra-nanoparticle pore system (originated by the template and porogen effects of the micelles) is defined by regular mesopores organized in a pseudohexagonal disordered array. In fact, all of the XRD patterns display one strong and broad diffraction peak and a small shoulder in the low angle region, which can be indexed (on the basis of an MCM-41-like hexagonal cell) to the (100) and (110) and (200) overlapped reflections, respectively (Figure 2 and Table 1). The change of surfactant gives rise to an evolution in the XRD patterns: the peak positions appear shifted at lower 2θ values as the surfactant tail length increases, which is consistent with a concomitant cell expansion. Then, a modulation in steps of around 0.4−0.5 nm is achieved in the intra-nanoparticle mesopore system (while maintaining the NBS organization).

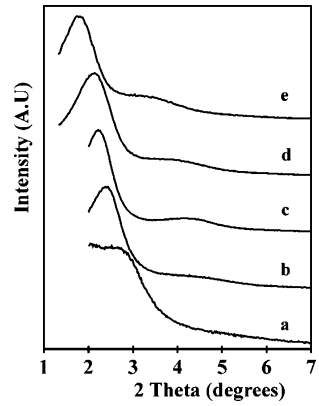

Figure 2. XRD patterns of (a) sample 1, (b) sample 2, (c) sample 3, (d) sample 4, and (e) sample 5.

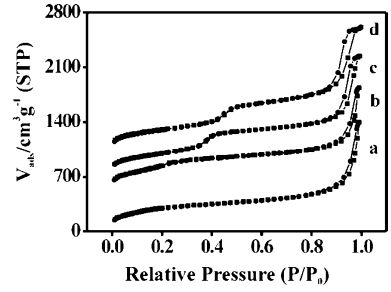

Figure 3. Representative N_2 adsorption desorption isotherms of (a) sample 1, (b) sample 2, (c) sample 4, and (d) sample 5.

The bimodal character of the final silicas is further illustrated by the N_2 adsorption−desorption isotherms (Figure 3 and Table 1). As can be noted, the curves show two well-defined adsorption steps. The first, at an intermediate relative pressure ($0.3 < P/P_0 < 0.5$), is characteristic of type IV isotherms and can be related to the capillary condensation of N_2 inside the intra-nanoparticle mesopores. The second step, at a high relative pressure ($P/P_0 > 0.8$), corresponds to the filling of the large pores among the primary nanoparticles. The XRD data correlate very well with the evolution observed in all of those aspects related to the first adsorption step ($P/P_0 < 0.5$). The BJH intraparticle pore size and pore volume regularly decrease (until the micropore range is reached) with the tail length. However, in contrast to previous results (where the NBS architecture was not preserved),[16] the characteristics of the interparticle large-pore system remain now practically unchanged, with pore size and volume values around 50 nm and 1.3 cm^3/g, respectively. We can consequently conclude that, for the first time, we have achieved a steeped control of the small intraparticle pores without concomitantly inducing significant effects on the particle size and the hierarchic architecture of the UVM-7-like silicas.

Interparticle Pore Control. Once the feasibility of modulating the small intraparticle mesopore system was proved, we focused our attention on the possibility of achieving an additional independent control of the large interparticle (textural) porosity. The generation of the large pore system can be viewed as resulting from the processes of aggregation of nanoparticles, which implies the establish-

ment of Si−O−Si covalent links among the primary particles. This aggregation is a sol−gel process that could be the result of base-catalyzed interparticle collisions.[22] Under this assumption, since the colliding primary nanoparticles ($(((C_xTMA)_mSi_{n+m}O_{3/2(n+m)}(OH)_nO_m)_{(s)}$) generated through equilibrium 1 have neutral (SiOH) and anionic (SiO^-) groups on their surface, we should have to control the condensation reactions among these Si moieties in order to modulate the textural large-pore system. Although these processes must be pH-dependent, the buffering effect due to the presence of triethanolamine in the reaction medium strongly limits the use of the pH as an effective tool. Moreover, changes in the pH could lead to a loss of the NBS nature.[14,16] Then, we have explored the efficiency of a different procedural variable to regulate the condensation processes: the addition to the reaction medium of variable amounts of alcohol as a cosolvent in order to modulate the dielectric constant of the medium. As we immediately show, the textural porosity becomes easily controllable by the addition of mixtures of water and ethanol to the starting solution of the reagents (silatranes and alkyltrimethilammonium surfactants). Indeed, as exemplified in Tables 1 ($z = 0$) and 2 ($z = 3$, 5, 10, 40, and 50) for the case of $C_{16}TMABr$, we have modified the ethanol molar content (z) from 0 to 50, while maintaining both the water amount (z $CH_3-CH_2-OH/180$ H_2O) and the surfactant to water proportions (calculated in each case according to the corresponding cmc value). Under these conditions of relatively low alcohol proportion ($0 \leq$ ethanol/water molar ratio ≤ 0.27) and maintaining a high $H_2O/Si = 90$ molar ratio, the effect on the hydrolysis of the silatrane precursors can be considered as negligible, in accordance with the alkoxisilane sol−gel chemistry.[23] Ethanol addition results in a gradual variation of the dielectric constant of the reaction medium.[24] The cooperative effect of triethanolamine and ethanol gradually reduces the dielectric constant of the medium until values of around 50 are reached ($z = 0$, $\varepsilon = 75$; $z = 3$, $\varepsilon = 68$; $z = 5$, $\varepsilon = 60$; $z = 10$, $\varepsilon = 57$; $z = 40$, $\varepsilon = 45$; $z = 50$, $\varepsilon = 41$), which subsequently favors in a progressive way the nanoparticle aggregation. The TEM and SEM images in Figure 4 confirm in practice the evolution of the aggregation processes as the ethanol content in the mother solution increases. A similar evolution of the aggregation level of the primary mesoporous nanoparticles with ethanol has been observed when other surfactants of the alkyl-trimethylammonium bromide family ($C_xTMA^+Br^-$, $x = 10$, 12, 14, 18) have been used as templates.

The selection of ethanol as a cosolvent is not arbitrary. In practice, besides the dielectric constant of the medium, the presence of alcohols can alter other physicochemical parameters affecting equilibrium 1. In effect, it is well-known that the concentration of surfactants in the form of micelles ($(C_xTMA^+Br^-)_m$) decreases rapidly as the alcohol concentration increases.[25] As indicated above, this decrease of the cmc values will affect the aggregation and dynamics of pure alkyltrimethil-ammonium surfactants and also the formation of silica mesostructures.[26] In order to preserve the NBS architecture (at least along a certain alcohol/water ratio), we have selected ethanol because this alcohol allows modification of the dielectric constant while inducing only minor changes in the cmc values. It must be indicated that the surfactant cmc values are relatively less affected by the addition of short-chain alcohols (such as methanol or ethanol) due to their low partition coefficients.[27]

The N_2 adsorption−desorption isotherms (Figure 5) confirm the bimodal or unimodal nature of the final solids, with

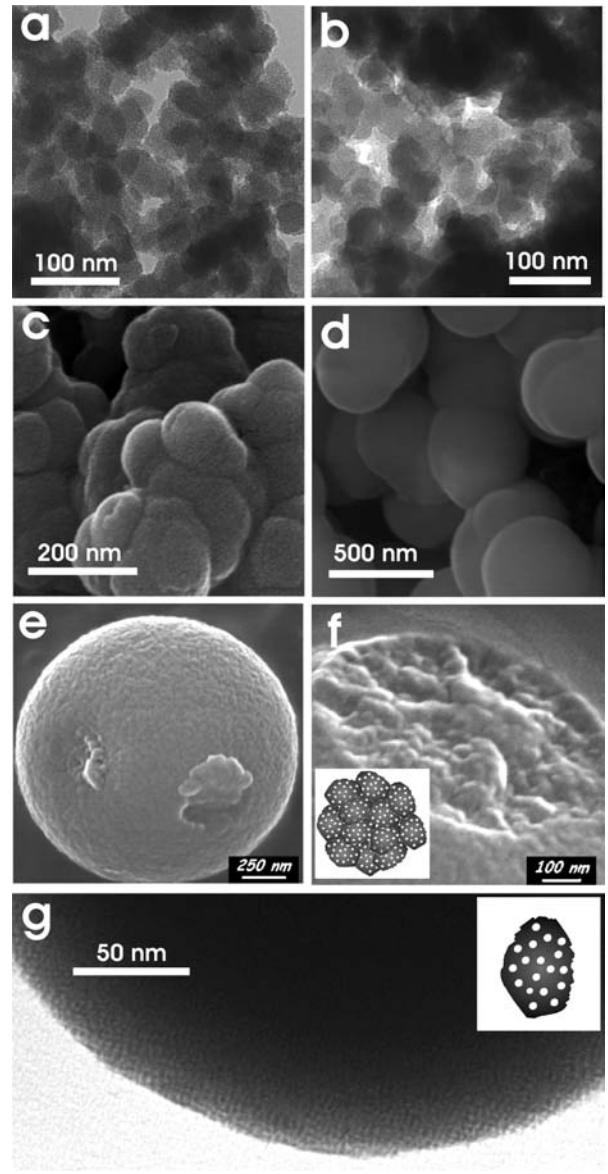

Figure 4. Micrographs of porous silicas synthesized with variable ethanol amounts. (a) Sample 6, (b) sample 7, (c) sample 8, (d) sample 9, (e and f) sample 10, and (g) detailed TEM image of sample 10.

(22) Iller, R. K. *The Chemistry of Silica. Solubility, Polymerization, Colloid and Surface Properties, and Biochemistry*; John Wiley & Sons: New York, 1979.
(23) Brinker, C. J.; Scherer, G. W. *Sol-Gel Science, The Physics and Chemistry of Sol-Gel Processing*; Academic Press, Inc.: London, 1990.
(24) Franks, F.; Ives, D. J. G. *Quart. Rev.* **1966**, *20*, 1.
(25) Wall, J. F.; Zukoski, C. F. *Langmuir* **1999**, *15*, 7432.
(26) Anderson, M. T.; Martin, J. E.; Odinek, J. G.; Newcomer, P. P. *Chem. Mater.* **1998**, *10*, 1490.
(27) Zana, R.; Yiv, S.; Strazielle, C.; Lianos, P. *J. Colloid Interface Sci.* **1981**, *80*, 208.

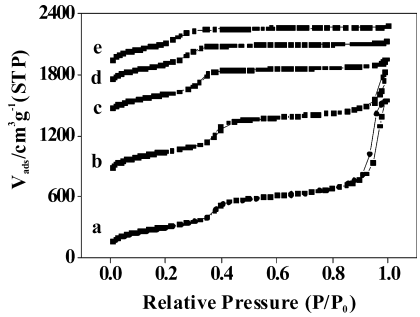

Figure 5. Representative N_2 adsorption desorption isotherms of (a) sample 6, (b) sample 7, (c) sample 8, (d) sample 9, and (e) sample 10.

a good correlation with the microscopy images. The evolution of the textural porosity takes place in a gradual way for ethanol molar contents ranging from 3 to 10, while the NBS architecture is clearly preserved only for ethanol molar contents lower than 10. Interparticle porosity disappears for ethanol molar contents higher than 10, as reflected by the unimodal N_2 adsorption−desorption isotherms recorded. In the limit, when the ethanol molar content ranges from 40 to 50, the solids appear as constructed from large mesoporous spheres with Stöber-like morphology (see Figure 4).

The large interparticle pores correspond to the voids generated in a continuous network of soldered nanoparticles. The nonordered nature of this large pore system is consistent with a formation mechanism, implying collision and the aggregation of primary nanoparticles, in which no supramolecular template able to transfer a certain organization participates. Then, this pore system shows a broad distribution centered in the boundary between meso- and macropores. Our strategy does not imply significant changes in the pore sizes. We observe broad pore size distributions with BJH pores in the 45−60 nm range. On the contrary, a fine modulation of the porosity, referred to as the large pore volume, is achieved. Thus, the BJH pore volume associated with these textural pores decreases in a regular way from 1.51 cm^3/g to 0.15 cm^3/g as the ethanol molar content increases from 3 to 10. The parallel and gradual evolution of the intraparticle pore sizes (from *ca.* 3.0 to 2.5 nm) with the ethanol content can be attributed to the micelle shrinkage induced by the changes in the reaction medium. In fact, a slight increase in the respective cmc values together with a certain micelle-size decrease is expected as the ethanol content increases.[28] In any case, this contraction of the small mesopores can be compensated by the addition of small amounts of micelle swelling agents such as TMB.

Regardless of the architecture of the final silica, from NBS to Stöber-like micrometric spheres, the TEM and SEM images in Figure 4 suggest that, in all cases, the surfactant-assisted mesoporous primary nanoparticles are the basic structural building blocks. This aspect is evident for NBS materials obtained from low-content ethanol solutions. In this case, we observe that the particle size increases from ca. 20−25 nm to 35−40 nm with the ethanol content (Figure 4a,b). This evolution could be related to the slight increase

(28) Anderson, M. T.; Martin, J. E.; Odinek, J. G.; Newcomer, P. P. *Chem. Mater.* **1998**, *10*, 311.

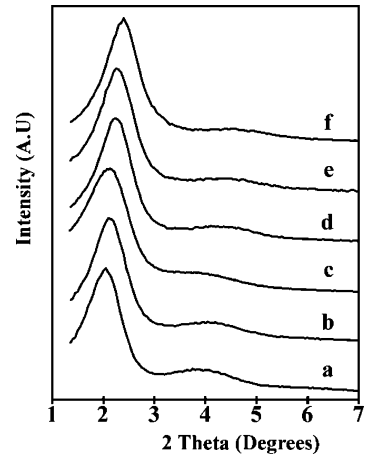

Figure 6. XRD patterns of (a) sample 4, (b) sample 6, (c) sample 7, (d) sample 8, (e) sample 9, and (f) sample 10.

of the cmc value of the surfactant with the ethanol content, which thwarts the complete precipitation of small nanoparticles and favors a certain particle growing from the reagents in solution. Dealing with the Stöber-like spheres, both TEM images and N_2 adsorption−desorption isotherms are consistent with their mesoporous character. Moreover, on the micrometric scale, the rough surfaces observed in the SEM micrographs (Figure 4c−f) suggest the existence of well-cemented mesoporous nanoparticles. Once the primary nanoparticles are aggregated, the subsequent particle growth (from the silica species and surfactant molecules in an ethanol-rich solution) completes as the sphere formation is cemented.

Finally, irrespective of the NBS or Stöber-like nature of the final silicas, the XRD patterns show a similar order in the intraparticle mesopore system. In fact, all materials display XRD patterns with one strong peak and one broad signal of relatively low intensity (Figure 6), which can be respectively associated with the (100) and the overlapped (110) and (200) reflections of an MCM-41-like hexagonal cell. These patterns are characteristic of hexagonal disordered mesoporous materials, and they only inform us about the existence of the intrananoparticle mesopore ("small" pores) system. The slight broadening of the (100) reflection (measured as the full width at half maximum) as the ethanol content increases indicates a progressive lowering of long-range order, which has also been documented for MCM-41 silicas.[25] This evolution could probably be due to the increased molecular disorder in the palisade layer of the resulting mixed surfactant−alcohol micelles generated through the replacement of surfactants by alcohols (with respect to the situation in the absence of alcohol).[27] On the other hand, the progressive evolution of the (100) peak toward low *d* spacing values as the ethanol content increases must be related to the above-mentioned alcohol-induced micelle shrinkage.[28] The presence of partial disordered intraparticle mesopores also is appreciated from the TEM images, both for NBS (Figure 4 a,b) and Stober-like porous particles (Figure 4g).

Intraparticle Pore System Order. Although the symmetry of the mesopore array is irrelevant for a majority of

Scheme 1. Proposed Reaction Mechanism to Explain the Different Growing for Ordered and Disordered NBS Materials

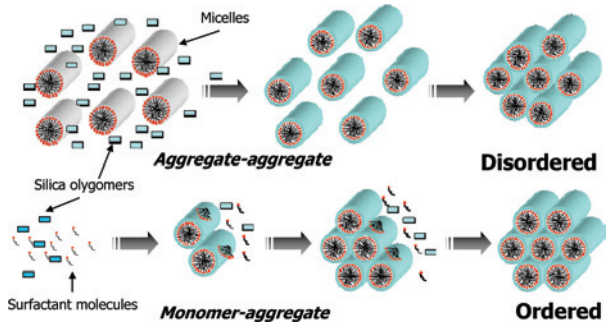

applications of M41S and related materials,[1] this is not the case in some concrete uses. For example, it becomes a fundamental requisite for optimizing the response and sensibility in a set of hybrid mesoporous sensing systems.[29] So, we have also explored the possibility of modulating the order degree in the intraparticle pore system. The preparation of mesoporous nanoparticles displaying hexagonal ordered pore arrays has been considered in a small number of previous works. As far as we know, the formation of such singular nanoparticles was detected for the first time by Mann and co-workers during the study of the nucleation and growth of MCM-41.[30] Also, more recent publications describe the synthesis of hexagonal ordered NBS materials by using a double surfactant system.[15e,f] Here, our purpose has been obtaining UVM-7-like materials including intraparticle mesopore systems with hexagonal ordered symmetry, but preserving simultaneously the capability of modulating both hierarchic pore systems (through the one-pot and one-surfactant approach we are dealing with).

Until this point, we have emphasized that our preparative conditions (including the use of variable tail-length surfactants or the addition of ethanol to the reaction medium) are consistent with the presence in solution of rodlike surfactant micelles when the silica−oligomers' formation goes on. Even more, we have imposed surfactant concentrations slightly higher than those corresponding to the respective cmc values. Under these conditions, we have proposed the formation of "silica-coated surfactant micelles" (through an S^+I^- mechanism, equilibrium 1) as primary building block nanoobjects.[6,7] Then, the growth of mesoporous nanoparticles would imply a cluster−cluster aggregation mechanism where the large supramolecular size of the building blocks hinders their organization in highly symmetric arrays (Scheme 1).[31] Hence, hexagonal disordered intraparticle mesopore systems are usually attained.

Our strategy to enhance the intraparticle mesopore symmetry is based on using more diluted systems (Table 3). The high dilution conditions now used affect both the inorganic and organic reagents implied in equilibrium 1 and also their cooperative self-assembling. At such high dilutions, the surfactant concentration is clearly lower than the corresponding cmc value. If so, the surfactant species in solution will be isolated molecules ($mC_xTMA^+Br^-$) instead of preorganized micelles ($(C_xTMA^+Br^-)_m$). Dealing with the inorganic species, a lower polymerization degree of the resulting silica oligomers is expected when compared to more concentrated solutions.[22] Then, we start from building blocks of relatively small size. There are several recent works demonstrating that silica mesophases can be synthesized even at extremely low surfactant concentrations. Indeed, Vautier-Giongo and Pastore[32] have reported on how silicate anions can induce C_{16}TMABr micellation at surfactant concentrations very distant from the cmc values. Also, Tajandra et al.[33] have prepared a very nice pseudophase diagram (concentration of C_{16}TMABr vs concentration of sodium silicate) showing that, regardless of the C_{16}TMABr concentration, it is possible to segregate a mesostructure at silica concentrations exceeding 5 mM. Accordingly, ordered silica mesophases could be isolated starting from hybrid micelles or molecular silica−surfactant complexes working at C_{16}TMABr concentrations higher or lower than the cmc value, respectively, without prejudice to the usually higher reaction yields attained in the first case. On the other hand, a simulation of the mesostructure formation process (using the off-lattice Monte Carlo method) supports the idea that ordered mesoporous materials can be isolated from micelles or isolated surfactant molecules.[34] Under these conditions, both the low dimension of the building blocks (which favors a more regular self-assembling)[31] and the fact that silica-induced micellation in the dilute regime leads to the growing and elongation of the micelles without significant entanglement[35] will propitiate the isolation of ordered silica. Very likely, the nanoparticle growth will take place now through a different cluster-monomer aggregation mechanism (Scheme 1).

Shown in Figure 7 are TEM images corresponding to a UVM-7 sample synthesized from a highly diluted solution (sample 12, $w = 2880$), while maintaining the Si/TEAH3 molar ratio (2:7) of the standard protocol (Table 3). As can be observed, the micrograph in Figure 7a confirms the preservation of the NBS topology (aggregation of mesoporous nanoparticles with large interparticle voids). Also, we can see in the magnified/high-resolution image in Figure 7b how the nanoparticles really present a hexagonal ordered mesopore array. This last feature is confirmed by the corresponding XRD pattern included in Figure 7. Thus, in the low angle domain, this pattern displays together with the (100) intense signal at least two other small (but well-resolved) peaks that can be assigned to the (110) and (200) reflections of an MCM-41-like hexagonal cell. Indeed, the high symmetry of the pore array plus the cluster-monomer growing mechanism result in spherical nanoparticles that

(29) Descalzo, A. B.; Jimenez, D.; Marcos, M. D.; Martínez-Máñez, R.; Soto, J.; El Haskouri, J.; Beltrán, D.; Amorós, P.; Borrachero, M. V. *Adv. Mater.* **2002**, *14*, 966.
(30) Sadasivan, S.; Fowler, C. E.; Khushalani, D.; Mann, S. *Agew. Chem., Int. Ed* **2002**, *114*, 2255.
(31) Berggren, A.; Palmqvist, A. E. C.; Holmberg, K. *Soft Matter* **2005**, *1*, 219.
(32) Vautier-Giongo, C.; Pastore, H. O. *J. Colloid Interface Sci.* **2006**, *299*, 874.
(33) Tjandra, W.; Yao, J.; Tam, K. C. *Langmuir* **2006**, *22*, 1493.
(34) Bhattacharya, A.; Mahanti, S. D. *J. Phys.: Condens. Matter* **2001**, *13*, 861.
(35) Lee, Y. S.; Surjadi, D.; Rathman, J. F. *Langmuir* **2000**, *16*, 195.

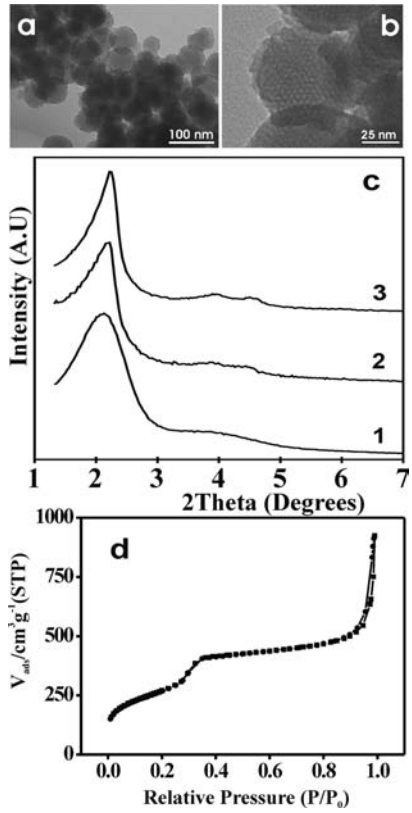

Figure 7. (a, b) Micrographs of hexagonal ordered UVM-7 materials (sample 12). (c) Evolution of the XRD pattern as the ethanol content increases: (1) sample 4 (without ethanol), (2) sample 11, and (3) sample 12. (d) N_2 adsorption−desorption isotherm of sample 12.

could be considered as a nanosized version of the porous Stöber-like particles mentioned above. On the other hand, their slightly higher dimensions (when compared to the above-described NBS silicas) can be understood taking into account that we are far away from supersaturation conditions, and a certain Ostwald-ripening growing is consequently expected. Nevertheless, the use of atrane precursors and thriethanolamine cosolvent allows maintenance of the optimum pH conditions (high hydrolysis and condensation rates, eqs 2 and 3). Then, all of the chemical requisites concerning the inorganic counterpart which favor the NBS topology are preserved. In practice, as indicated above, the only difference with regard to the evolution of equilibrium 1 concerns the pre-existence of surfactant micelles.

The preservation of the NBS typical architecture is further illustrated by the N_2 adsorption−desorption isotherms in Figure 7d. As can be noted, the curve shows two well-defined adsorption steps. The first, at an intermediate relative pressure ($0.3 < P/P_0 < 0.5$) can be associated with the intraparticle mesopore capillary condensation, and the second step, at a high relative pressure ($P/P_0 > 0.8$), corresponds to the filling of the large pores among the primary nanoparticles.

This strategy for increasing the intraparticle pore system symmetry through dilution has been successfully applied when using surfactants with medium or long tail lengths ($14 \leq x \leq 18$). However, as the surfactant aggregation number (m in equilibrium 1; $(C_xTMA^+Br^-)_m$) decreases ($x = 10$, 12),[19,20] the dilution strategy leads to the formation of mesoporous large microparticles (with a loss of the NBS morphology) or even to a lack of mesostructure stabilization.

Concluding Remarks

We present here the first unified preparative strategy that allows control in an independent way of the intra- and interparticle pore systems in bimodal silicas constructed from the aggregation of nanoparticles. Our preparative protocol has been designed on the basis of well-founded physicochemical concepts affecting both the inorganic and organic counterparts and also the interaction among them: the hydrolysis and condensation of Si species, the micellation processes of the surfactants, and the influence of the reaction media (dielectric constant changes). This relatively straightforward approach has not been outlined until now. We propose that, in order to control the morphological characteristics of mesoporous silicas with reasonable yields, it is adequate to select surfactant concentrations close to cmc (taking into account the tail length), and also to choose the silica−solvent system variables, paying attention to parameters controlling the processes of nucleation and growth of the "composite" mesostructured crystals.

We have benefited from our own experience in order to propose this methodology: this one-pot and one-surfactant approach allows the preparation of NBS-like materials in an easy and reproducible way by simple control of the concentration of the reagents in the general system 2Si/7 TEAH3/y C_xTMABr/z ethanol/w H_2O. Moreover, the achieved modulation of the pores can be combined with the large compositional control typical of the "atrane method",[17] which overcomes problems associated with the great reactivity differences among silica and nonsilica species. In fact, UVM-7-like solids can be easily modified through one-pot syntheses and variable contents of different heteroelements, and organic groups can be included without significant morphological changes.[9,14,36]

Acknowledgment. We thank the MEC (CTQ2006-15456-C04-03 grant) for support. J.E.H. and L.F. thank the MEC for Ramón & Cajal contracts.

IC800893A

(36) (a) El Haskouri, J.; Ortízde Zárate, D.; Pérez, F.; Cervilla, A.; Guillem, C.; Latorre, J.; Marcos, M. D.; Beltrán, A.; Beltrán, D.; Amorós, P. *New J. Chem.* **2002**, *26*, 1093. (b) El Haskouri, J.; Ortízde Zárate, D.; Guillem, C.; Beltrán, A.; Beltrán, D.; Caldés, M.; Latorre, J.; Amorós, P. *Chem. Mater.* **2002**, *14*, 4502. (c) Ortiz de Zárate, D.; Gómez-Moratalla, A.; Guillem, C.; Beltrán, A.; Latorre, J.; Beltrán, D.; Amorós, P. *Eur. J. Inorg. Chem.* **2006**, 2572. (d) Huerta, L. J.; Amorós, P.; Beltrán, D.; Cortés-Corberán, V. *Catal. Today* **2006**, *117*, 180.